Sciencexpress Research Articles

EMBARGOED UNTIL 2:00 PM US ET THURSDAY, 20 SEPTEMBER 2012

Detecting Causality in Complex Ecosystems

George Sugihara,[1]* Robert May,[2] Hao Ye,[1] Chih-hao Hsieh,[3] Ethan Deyle,[1] Michael Fogarty,[4] Stephan Munch[5]

[1]Scripps Institution of Oceanography, University of California, San Diego, 9500 Gilman Drive, La Jolla, CA 92093, USA. [2]Department of Zoology, University of Oxford, Oxford OX1 3PS, UK. [3]Institute of Oceanography, National Taiwan University, No. 1, Sec. 4, Roosevelt Road, Taipei 106, Taiwan. [4]Northeast Fisheries Science Center, National Oceanic and Atmospheric Administration, 166 Water Street, Woods Hole, MA 02543, USA. [5]Southwest Fisheries Science Center, National Oceanic and Atmospheric Administration, 110 Shaffer Road, Santa Cruz, CA 95060, USA.

*To whom correspondence should be addressed. E-mail: gsugihara@ucsd.edu

Identifying causal networks is important for effective policy and management recommendations on climate, epidemiology, financial regulation, and much else. Here we introduce a method, based on nonlinear state space reconstruction, that can distinguish causality from correlation. It extends to nonseparable weakly connected dynamic systems (cases not covered by the current Granger causality paradigm). The approach is illustrated both by simple models (where, in contrast to the real world, we know the underlying equations/relations and so can check the validity of our method) and by application to real ecological systems, including the controversial sardine-anchovy-temperature problem.

Identifying causality (*1*) in complex systems can be difficult. Contradictions arise in many scientific contexts where variables are positively coupled at some times and at other times appear unrelated or even negatively coupled depending on system state (movie S1). Baltic Sea fisheries, for example, are known to exhibit radically different dynamic control regimes (top down versus bottom up) depending on the threshold abundance of planktivores, causing the correlations between fish abundance and zooplankton time series to change sign (*2*). Such state-dependent behavior is a defining hallmark of complex nonlinear systems (*3*, *4*), and nonlinearity is ubiquitous in nature (*3–11*).

Ephemeral or "mirage" correlations are common in even the simplest nonlinear systems (*7*, *11–13*), such as shown in Fig. 1 for two coupled first-order nonlinear difference equations that exhibit chaotic behavior (*14*).

$$\begin{aligned} X(t+1) &= X(t)\left[r_x - r_x X(t) - \beta_{x,y} Y(t)\right] \\ Y(t+1) &= Y(t)\left[r_y - r_y Y(t) - \beta_{y,x} X(t)\right] \end{aligned} \quad (1)$$

When this happens variables that are positively coupled for long periods, can spontaneously become anti-correlated or decoupled. Such behavior is a common problem in fitting models to observational data (*15*).

Although correlation is neither necessary nor sufficient to establish causation, it remains deeply ingrained in our heuristic thinking (*8*, *13*, *16*, *17*). Thus, one might conclude (incorrectly) that because the coupled variables in Fig. 1 show no long-term correlation, there is no causal link. With increasing recognition that nonlinear dynamics are ubiquitous, and that relationships among variables will depend on system state, the use of correlation to infer causation becomes truly difficult.

An alternative approach, Granger causality (GC) (*18*), provides a framework for investigating causal linkages among time series variables, where predictability as opposed to correlation is used to establish causation. GC is recognized as the primary advance on the causation problem since Berkeley (*1*). Variable X is said to "Granger cause" Y if the predictability of Y (in some exact idealized model) declines when X is removed from the universe of all possible causative variables, U (*18*). The key requirement of Granger is separability, namely that information about a causative factor is unique to that variable (e.g., information about predator effects is not contained in time series for the prey). Separability is satisfied in most linear systems, and GC has been useful for stochastic systems, for nonlinear systems exhibiting stable points or limit cycles (linear dynamics that do not depend on system state), and for detecting interactions between strongly-coupled variables in nonlinear systems.

However, as Granger (*18*) realized early on, this approach may be problematic in general nonlinear dynamic systems (especially with weak to moderate coupling). For example, ambiguous results are obtained for the system in Fig. 1 (see GC calculations S1). This is because separability is not satisfied in such systems. That is to say, if X is a cause for Y, information about X will be redundantly present in Y itself, and cannot formally be removed from U—a consequence of Takens' Theorem (*19*, *20*). To see this, note that Eq. 1 could be equivalently re-written as a model for $X(t + 1)$ in terms of $X(t)$ and $X(t - 1)$ (see box S1 for a worked example). Doing so makes the information from $Y(t)$ completely redundant—it can be removed without affecting our ability to predict $X(t + 1)$. When Granger's definition is violated, GC calculations are no longer valid, leaving open the question of detecting causation in such systems.

In addition to non-separability, ecosystems differ from the systems typically studied with Granger's approach in other significant ways. First, in ecosystem dynamics, weak to moderate coupling is the norm. McCann (*21*) and others have developed a strong case for the ubiquity of weak coupling in ecological food webs and have demonstrated the importance of weak to moderate coupling for system stability. Second, ecosystems are typically subject to forcing by external driving variables such as temperature, precipitation, and upwelling [e.g., (*6*, *22*)]. Because many species share similar abiotic environments, this can lead to correlations and apparent synchrony among non-interacting species [e.g., the Moran effect (*23*)], complicating the task of identifying coupling among ecosystem components. It is therefore important in ecology to have methods that: (i) address non-separable nonlinear systems, (ii) identify weakly coupled variables, and (iii) distinguish the dynamics of interactions among individual species from the effects of shared driving variables.

Here we examine an approach aimed specifically at identifying causation in ecological time series: cases not covered by GC. We demonstrate the principles of our approach with simple model examples, showing that the method is effective at distinguishing species interactions from the effects of shared driving variables. Finally, we apply the method to ecological data from experimental and field studies that fall outside Granger's framework, showing how it distinguishes top-down from bottom-up control in the classic *Paramecium-Didinium* experiment, and clarifies the ongoing debate about the nature of interactions among sardine, anchovy and sea surface temperature in the California Current ecosystem.

Our approach is not competing with the many effective methods that use GC (see supplementary text); rather it is specifically aimed at a class

of system not covered by GC. GC calculations S1 to S5 verify that GC does not apply to this class of system.

Dynamic causation and CCM. In dynamical systems theory, time series variables (say X and Y) are causally linked if they are from the same dynamic system (*4*, *19*, *20*), thereby sharing a common attractor manifold $\mathbf{M}$ (movies S1 to S3 illustrate this idea). This means that each variable can identify the state of the other (*3*, *19*, *20*, *24*, *25*) (e.g., information about past prey populations can be recovered from the predator time series, and vice versa). Additionally, when one variable (say X) is a stochastic environmental driver of a population variable Y, information about the states of X can be recovered from Y, but not vice-versa (e.g., fish time series can be used to estimate weather but not vice versa), which runs counter to Granger's intuitive scheme (see explanation in box S1).

Our alternative approach, convergent cross mapping (CCM), tests for causation by measuring the extent to which the historical record of Y-values can reliably estimate the state of X. This can only happen if X is causally influencing Y. In more detail, CCM looks for the signature of X in Y's time series by seeing if there is a correspondence between the "library" of points in the attractor manifold built from Y, $\mathbf{M}_Y$, and points in the X manifold, $\mathbf{M}_X$; these two manifolds are constructed from lagged-coordinates of the time series variables Y and X respectively (*3*, *19*, *24*) (movies S1 and S2).

Essentially, the idea is to see if nearby points on $\mathbf{M}_Y$ correspond temporally to nearby points on $\mathbf{M}_X$; and more specifically, if the time indices of nearby points on $\mathbf{M}_Y$ can be used to identify nearby points on $\mathbf{M}_X$. If so, then one can use Y to estimate states of X and visa versa. This procedure is illustrated in Fig. 2 and movie S3, with full technical details including an algorithm in (*26*).

Note that CCM is related to the general notion of cross prediction (*3*, *25*) but with important differences. First, CCM estimates "states" across variables and does not forecast how the system "evolves" on the manifold. This eliminates possible information loss from chaotic dynamics (Lyapunov divergence), and accommodates non-dynamic (i.e., random) variables. More importantly, CCM involves convergence, a key property that distinguishes causation from simple correlation. Convergence means that cross-mapped estimates improve in estimation skill with time series length, L (sample size used to construct a library) (Fig. 3A, fig. S2, and box S1). With more data, the trajectories defining the attractor fill in and become dense, resulting in closer nearest neighbors and declining estimation error (a higher correlation coefficient) as L increases (Fig. 2). Thus, CCM is a necessary condition for causation. Indeed, it can be shown that failing to account for convergence explains conflicting results reported in the literature with related methods (supplementary text) (fig. S5).

In practical applications, where shadow manifolds are low dimensional approximations of the true system, convergence will be limited by observational error, process noise and time series length, L. Thus, with limited or noisy field data CCM is demonstrated by predictability that increases with L (fig. S3). See (*26*) for a discussion of data requirements.

Framework for identifying causation, case i: Bidirectional causality via functional coupling. Bidirectional causality is analogous to the concept of "feedback" between two time series described by Granger (*18*) and is the primary case covered by Takens (*19*). Simply put, if variables are mutually coupled (e.g., predator and prey), they will cross map in both directions (Fig. 3A and fig. S1A). Thus, each variable can be estimated from the other. Figure 3B gives examples of the general case *i*.

Notice that as the strength of coupling increases, information becomes more distinct in the affected variables. As a result, manifolds built from time series of the affected variables will contain stronger historical signatures of the causes. In Fig. 1 (Eq. 1), for example, where $\beta_{y,x} >> \beta_{x,y}$ the much stronger effect of species X on species Y implies faster convergence for predicting species X than species Y (Fig. 3A). Thus, all things equal, the relative skill of cross mapping can indicate the relative magnitude of causative effect (Fig. 3B).

Framework for identifying causation, case ii: Unidirectional causality. Here species X influences the dynamics of Y, but species Y has no effect on X (Fig. 3C, fig. S1B, and box S1). This could describe an amensal or comensal relationship, or where X represents external environmental forcing.

Figure 3C examines the system (1) when $\beta_{x,y} = 0$. Note that with moderately strong forcing (from $\beta_{y,x}$), even though $\beta_{x,y} = 0$ there may still be partial cross mapping of Y arising from the contemporaneous dependence of Y on X. However, this statistical effect is not convergent (shown by the asymptotic level curves with respect to L in Fig. 3E). With extremely strong forcing, the intrinsic dynamics of the forced variable can become subordinate to the forcing variable, leading to the well-studied phenomenon of "synchrony" (*27*). The red plateau in Fig. 3E shows that bidirectional convergence can occur with strong forcing. Thus, strong forcing (synchrony) must be ruled out for CCM to unequivocally imply bidirectional coupling, though it still implies membership to a common dynamic system.

Transitivity. Note that causation is transitive (eg., if foxes prey on rabbits, and rabbits eat grass, then foxes and grass are causally linked). More formally, $X \Leftrightarrow Y \Leftrightarrow Z$ implies $X \Leftrightarrow Z$, whether or not X and Z interact directly. Similarly, for unidirectional forcing, $X \Rightarrow Y$ and $Y \Rightarrow Z$, implies $X \Rightarrow Z$. Transitivity provides the basis for extending CCM to larger interaction networks, enabling us to distinguish variables that are coupled from those sharing a common driver. This is illustrated with two model examples below.

Complex model examples: External forcing of non-coupled variables. Consider the case where two species, X and Y, do not interact, but are both moderately forced by a common environmental variable Z (Example 1 schematic in Fig. 4A). This occurs commonly in ecological systems [the Moran effect (*23*)] and is a case that remains problematic in studies of causation. Here we expect cross mapping between species X and Y to fail because there is no information flow between variables, although information about the external forcing variable (Z) should still be recoverable from X and Y.

In fisheries for example, non-interacting populations with common peak recruitment years due to favorable environmental conditions may be correlated even though they do not interact. The simple fisheries model in Fig. 4B illustrates this situation (*26*), where although the significant cross correlation between species suggests that they might be coupled, cross mapping shows no evidence of convergence, proving that they are not coupled. This example demonstrates that the method can distinguish coupled dynamics from a simple correlation produced by shared driving variables.

Figure 4C provides an interesting further illustration of the method with a more complex five-species model [schematic in Fig. 4A, model details in (*26*)]. In this example, species 1, 2, and 3 represent a mutually interacting guild that externally force species 4 and 5, while 4 and 5 do not influence any other species. Species 1, 2, and 3 are akin to Z in the discussion above, with 4 and 5 akin to the externally forced non-coupled pair X and Y. Figure 4C shows that CCM is able to deduce the correct network of interactions getting all bidirectional and unidirectional links correct (as well as their relative magnitudes).

Real world examples: Demonstration with ecological data. Keep in mind that attractors constructed from real data are approximations of dynamics occurring in higher dimensions. Thus, although observational error and process noise will limit the level of convergence attainable, low dimensional approximations can still produce significant cross map estimates of causal effects.

Bidirectional causation in an experimental predator-prey system. We apply the analysis to time series from the classic experimental predator-prey system, first studied in the 1920's by Gause, involving

Didinium (predator) and *Paramecium* (prey), and later improved by Veilleux (*28*). Methodological details in (*26*).

The results in Fig. 5A suggest bidirectional coupling (case *i*), which accords with what is known. Moreover, the higher level of skill in cross mapping *Didinium* from the *Paramecium* time series than the reverse (Fig. 5B) suggests stronger top-down control by the predator, *Didinium*, than bottom-up control by the prey, *Paramecium*. This finding is consistent with the experimental protocol and illustrates asymmetrical bidirectional coupling (case *i*).

Complex causation in the sardine-anchovy system. Here we examine the relationship between Pacific sardine (*Sardinops sagax*) landings, Northern anchovy (*Engraulis mordax*) landings, and sea-surface temperature (SST) measured at Scripps Pier and Newport Pier (Fig. 5C).

Competing hypotheses have been advanced to explain the pattern of alternating dominance of sardine and anchovy across global fisheries on multidecadal time scales. While the observed reciprocal abundance levels (Fig. 5A) resonates with ecological competition as an underlying mechanism, global synchrony in sardine and anchovy stanzas (*29*) suggests the operation of large-scale environmental forcing coupled with species-specific differences in optimal temperature levels. Recent evidence of regime-like behavior in these systems suggests the operation of nonlinear processes (*10*).

Similar to the global pattern, in California, 20th century landings of Pacific sardine (*Sardinops sagax*) and Northern anchovy (*Engraulis mordax*) show one population peaking when the other is depressed. While Murphy and Isaacs (*30*) hypothesized that the species act in direct competition, Lasker and MacCall (*31*) argued that the species react differently to common large-scale environmental forcing. Moreover, paleoecological time series based on fish scales preserved in the anoxic sediments of the Santa Barbara basin revealed that the negative cross-correlation witnessed in the 20th century disappears in these longer time series (*32*). Correlation with environmental factors has also been elusive. Jacobson and MacCall (*33*) detected correlation between three-year running averages of the Scripps Pier sea surface temperature (SST) and sardine recruitment and spawning stock size using two approaches (a generalized additive model and a linearized Ricker stock-recruitment model with environmental terms). However, when the analysis was expanded to include recent stock assessments from 1992-2009, the relationships vanished (*34*). Though there are many possible explanations, such changes in correlation across different periods are consistent with nonlinear dynamics and mirage correlation.

We address this controversy using the same analytical protocol used for the *Didinium-Paramecium* example (*26*). The results in Fig. 5D show no significant cross-map signal between sardine and anchovy landings, indicating that sardines and anchovies do not interact (are not dynamically coupled). In addition, as expected, there is no detectable signature from either sardine or anchovy in the temperature manifold– obviously neither sardines nor anchovies affect SST. However there is significant asymmetric CCM between sardines and SST as well as between anchovies and SST (Fig. 5, E and F), meaning that temperature information is encoded in both fishery time series. The recoverable temperature signature reveals a weak coupling of temperature to sardines and anchovies. Thus, although sardines and anchovies are not actually interacting they are weakly forced by a common environmental driver, for which temperature is at least a viable proxy. Note that because of transitivity, temperature may be a proxy for a group of driving variables (i.e., temperature may not be the most proximate environmental driver). Our finding that SST influences sardine (Fig. 5, E and F) is consistent with earlier findings of Jacobson and MacCall (*33*). Supporting evidence with other fishery-independent data are provided in the supplementary text (figs. S3 and S4).

Finally, it is important to note that the measurable nonlinear coupling of temperature to sardines stocks, means that the effect of temperature varies with system state. Therefore, contrary to the current regulatory framework for sardines, a fixed temperature index will not suffice for sound management decisions. Rather a dynamic (state-dependent) rule involving temperature is required.

Final remarks on nonseparability. One of the fundamental ideas in this work is that when causation is unilateral, $X \Rightarrow Y$ (X drives Y as in case *ii*), then it is possible to estimate X from Y, but not Y from X. This runs counter to intuition (and GC), and suggests that if the weather drives fish populations, for example, we can use fish to predict the weather but not vice versa.

To further clarify how this works, consider the 2-species logistic model described earlier (Eq. 1). We can recover the cross map dynamics algebraically by rearranging Eq. 1 to give expressions for $Y(t)$ and $X(t)$, substituting these back into Eq. 1, and solving for $X(t)$ in terms of $Y(t)$ and $Y(t-1)$ (and vice versa, see the worked example in box S1).

The parameter $\beta_{x,y}$ governs the sensitivity of X to changes in Y. As $\beta_{x,y}$ approaches 0, X drives Y unidirectionally and the cross map estimate of X remains well-behaved. But the cross map model for Y has a singularity when $\beta_{x,y} = 0$. Hence, cross mapping allows the driver to be reconstructed from the driven variable, but not the other way around.

Finally, because Eq. 1 can be algebraically rearranged as a model for $X(t+1)$ purely in terms of $X(t)$ and $X(t-1)$, the information from Y becomes redundant and can be removed without affecting our ability to predict $X(t+1)$. Thus, GC would suggest (incorrectly!) that Y does not cause X (see GC calculation S1).

Summary. Despite the fundamental problems raised in Berkeley's 1710 "*A treatise on principles of human knowledge*," (*1*) correlation remains the analytical standard of modern science. This has become more difficult to justify with increasing recognition that nonlinear dynamics are ubiquitous. Apparent relationships among variables can switch spontaneously in nonlinear systems due to mirage correlations or a threshold change in regime, and correlation can lead to incorrect and contradictory hypotheses. Growing recognition of the prevalence and importance of nonlinear behavior calls for a better criterion for evaluating causation where experimental manipulation is not possible.

Granger causality addresses Berkeley's issues by using prediction rather than correlation as the criterion for causation in time series. This idea assumes that causes can be separated from effects, so that a variable is identified as causative if prediction skill declines when that variable is removed. This is a powerful idea for separable linear systems (especially purely stochastic systems); however it is not defined for all systems, and in particular not for general nonlinear dynamic systems where Takens' Theorem applies (*19*, *20*). To address these systems, we examine an approach that exploits non-separability by using CCM to test for membership to a common dynamical system. CCM is not a method competing with GC, but deals with a class of system often found in ecological study where GC is simply not applicable. Thus it is not surprising that as a further check, the GC calculations for all the model and real data examples considered in this work were largely unsuccessful (table S2 and GC calculations S1 to S5).

Although many empirical measures of species interactions exist (e.g., inferring interaction proxies from diet matrices), we suggest that causation inferred from time series information provides a "bottom-line" picture of interactions that is more direct than those possible with proxies. The ability to resolve causal networks from their dynamical behavior has implications for system identification and ecosystem based management, particularly where it is important to know which species interact as a group and need to be considered together. In resource management as elsewhere, accurate knowledge of the causal network can be essential for avoiding unforeseen consequences of regulatory actions.

References and Notes

1. G. Berkeley, A Treatise on Principles of Human Knowledge (1710).
2. M. Casini *et al*., Trophic cascades promote threshold-like shifts in pelagic marine ecosystems. *Proc. Natl. Acad. Sci. U.S.A.* **106**, 197 (2009). doi:10.1073/pnas.0806649105 Medline
3. G. Sugihara, R. M. May, Nonlinear forecasting as a way of distinguishing chaos from measurement error in time series. *Nature* **344**, 734 (1990). doi:10.1038/344734a0 Medline
4. P. A. Dixon, M. J. Milicich, G. Sugihara, Episodic fluctuations in larval supply. *Science* **283**, 1528 (1999). doi:10.1126/science.283.5407.1528 Medline
5. W. A. Brock, C. L. Sayers, Is the business cycle characterized by deterministic chaos? *J. Monet. Econ.* **22**, 71 (1988). doi:10.1016/0304-3932(88)90170-5
6. B. T. Grenfell *et al*., Noise and determinism in synchronized sheep dynamics. *Nature* **394**, 674 (1998). doi:10.1038/29291
7. A. Mysterud, N. C. Stenseth, N. G. Yoccoz, R. Langvatn, G. Steinheim, Nonlinear effects of large-scale climatic variability on wild and domestic herbivores. *Nature* **410**, 1096 (2001). doi:10.1038/35074099 Medline
8. C. H. Hsieh, S. M. Glaser, A. J. Lucas, G. Sugihara, Distinguishing random environmental fluctuations from ecological catastrophes for the North Pacific Ocean. *Nature* **435**, 336 (2005). doi:10.1038/nature03553 Medline
9. G. I. Bischi, C. Chiarella, L. Gardini, Eds., *Nonlinear Dynamics in Economics, Finance and Social Sciences* (Springer, Berlin, 2010).
10. D. A. S. Patil, B. R. Hunt, J. A. Carton, Identifying low-dimensional nonlinear behavior in atmospheric data. *Mon. Weather Rev.* **129**, 2116 (2001). doi:10.1175/1520-0493(2001)129<2116:ILDNBI>2.0.CO;2
11. T. T. Lo, H. H. Hsu, Change in the dominant decadal patterns and the late 1980s abrupt warming in the extratropical Northern Hemisphere. *Atmos. Sci. Lett.* **11**, 210 (2010). doi:10.1002/asl.275
12. X. Rodo, M. Pascual, G. Fuchs, A. S. G. Faruque, ENSO and cholera: A nonstationary link related to climate change? *Proc. Natl. Acad. Sci. U.S.A.* **99**, 12901 (2002). doi:10.1073/pnas.182203999 Medline
13. B. K. Wagner *et al*., Large-scale chemical dissection of mitochondrial function. *Nat. Biotechnol.* **26**, 343 (2008). doi:10.1038/nbt1387 Medline
14. A. L. Lloyd, The coupled logistic map: A simple model for the effects of spatial heterogeneity on population dynamics. *J. Theor. Biol.* **173**, 217 (1995). doi:10.1006/jtbi.1995.0058
15. Committee on Major U.S. Oceanographic Research Programs, National Research Council, *Global Ocean Science: Toward an Integrated Approach* (National Academies Press, Washington, DC, 1999).
16. Y. Chen, S. L. Bressler, M. Ding, Frequency decomposition of conditional Granger causality and application to multivariate neural field potential data. *J. Neurosci. Methods* **150**, 228 (2006). doi:10.1016/j.jneumeth.2005.06.011 Medline
17. R. M. May, S. A. Levin, G. Sugihara, Complex systems: Ecology for bankers. *Nature* **451**, 893 (2008). doi:10.1038/451893a Medline
18. C. W. J. Granger, Investigating causal relations by econometric models and cross-spectral methods. *Econometrica* **37**, 424 (1969). doi:10.2307/1912791
19. F. Takens, in *Dynamical Systems and Turbulence*, D. A. Rand, L. S. Young, Eds. (Springer-Verlag, New York, 1981), pp. 366–381.
20. E. R. Deyle, G. Sugihara, Generalized theorems for nonlinear state space reconstruction. *PLoS ONE* **6**, e18295 (2011). doi:10.1371/journal.pone.0018295 Medline
21. K. McCann, A. Hastings, G. R. Huxel, *Nature* **395**, 794 (1998). doi:10.1038/27427
22. C. H. Hsieh *et al*., Time series analyses reveal transient relationships between abundance of larval anchovy and environmental variables in the coastal waters southwest of Taiwan. *Fish. Oceanogr.* **18**, 102 (2009). doi:10.1111/j.1365-2419.2008.00498.x
23. P. A. P. Moran, The statistical analysis of the Canadian Lynx cycle. *Aust. J. Zool.* **1**, 291 (1953). doi:10.1071/ZO9530291
24. N. H. Packard, J. P. Crutchfield, J. D. Farmer, R. S. Shaw, Geometry from a time series. *Phys. Rev. Lett.* **45**, 712 (1980). doi:10.1103/PhysRevLett.45.712
25. F. A. Ascioti, E. Beltrami, T. O. Carroll, C. Wirick, Is there chaos in plankton dynamics? *J. Plankton Res.* **15**, 603 (1993). doi:10.1093/plankt/15.6.603
26. See supplementary materials on *Science* Online.
27. K. Josic, Synchronization of chaotic systems and invariant manifolds. *Nonlinearity* **13**, 1321 (2000). doi:10.1088/0951-7715/13/4/318
28. B. G. Veilleux, thesis, University of Alberta (1976).
29. R. A. Schwartzlose *et al*., Worldwide large-scale fluctuations of sardine and anchovy populations. *S. Afr. J. Mar. Sci.* **21**, 289 (1999). doi:10.2989/025776199784125962
30. G. I. Murphy, J. D. Isaacs, Species replacement in marine ecosystems with reference to the California current. *Minutes of Meeting Marine Research Committee* **7**, 1 (1964).
31. R. Lasker, A. MacCall, New ideas on the fluctuations of the clupeoid stocks off California. In *Proceedings of the Joint Oceanographic Assembly, Halifax, August 1982: General Symposia* (Department of Fisheries and Oceans, Ontario, 1983), pp. 110–120.
32. T. R. Baumgartner, A. Soutar, V. Ferreira-Bartrina, *CCOFI Rep.* **33**, 24 (1992).
33. L. D. Jacobson, A. D. MacCall, Stock-recruitment models for Pacific sardine (*Sardinops sagax*). *Can. J. Fish. Aquat. Sci.* **52**, 566 (1995). doi:10.1139/f95-057
34. S. McClatchie, R. Goericke, G. Auad, K. Hill, Re-assessment of the stock-recruit and temperature-recruit relationships for Pacific sardine (*Sardinops sagax*). *Can. J. Fish. Aquat. Sci.* **67**, 1782 (2010). doi:10.1139/F10-101

Acknowledgments: The authors would like to acknowledge Stuart Sandin, Les Kaufman, Alec McCall, John Melack, John Schnute, Laura Richards, Andy Rosneberg, Michio Kumagai, Hui Liu, Irit Altman, Ben Fissel, Sarah Glaser, Ben Carr, Emily Klein, Laura Storch, Stephen Kealhofer, Monica Kogler and Charles Perretti, for their comments and assistance with this work. Peter Sugihara developed and produced the initial animations for movies S1 and S2. This work received financial support from NSF DEB-1020372 (GS), NSF/NOAA CAMEO Award NA08OAR4320894 (GS), the McQuown Chair in Natural Science (GS), Sugihara Family Trust (GS), Quantitative Advisors http://qadvisors.com (GS), National Taiwan University (CH), National Science Council of Taiwan (CH), NSF Graduate Research Fellowships (HY and ED), and an EPA STAR Graduate Fellowship (ED).

Supplementary Materials

www.sciencemag.org/cgi/content/full/science.1227079
Materials and Methods
Figs. S1 to S5
Tables S1 to S26
Box S1
GC Calculations S1 to S5
References (*35–76*)
Movies S1 to S3

6 July 2012; accepted 4 September 2012

Published online 20 September 2012
10.1126/science.1227079

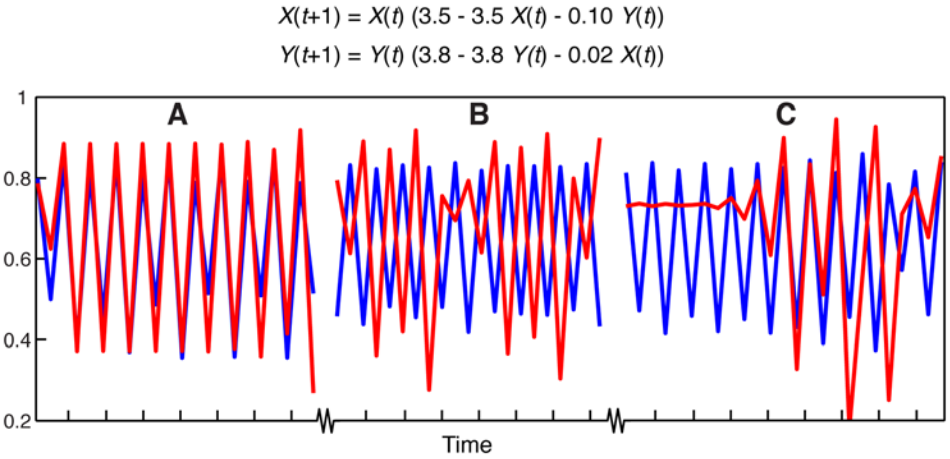

Fig. 1. Mirage correlations. (**A** to **C**) Three samples from a single run of a coupled 2-species nonlinear logistic difference system with chaotic dynamics. Variables *X* (blue) and *Y* (red) appear correlated in the first time segment (A), anti-correlated in the second time segment (B), and lose all coherence in the third time segment (C) with alternating interspersed periods of positive, negative, and zero correlation. Although the system is deterministic and dynamically coupled, there is no long-term correlation (n = 1000, ρ = 0.0054, p = 0.864).

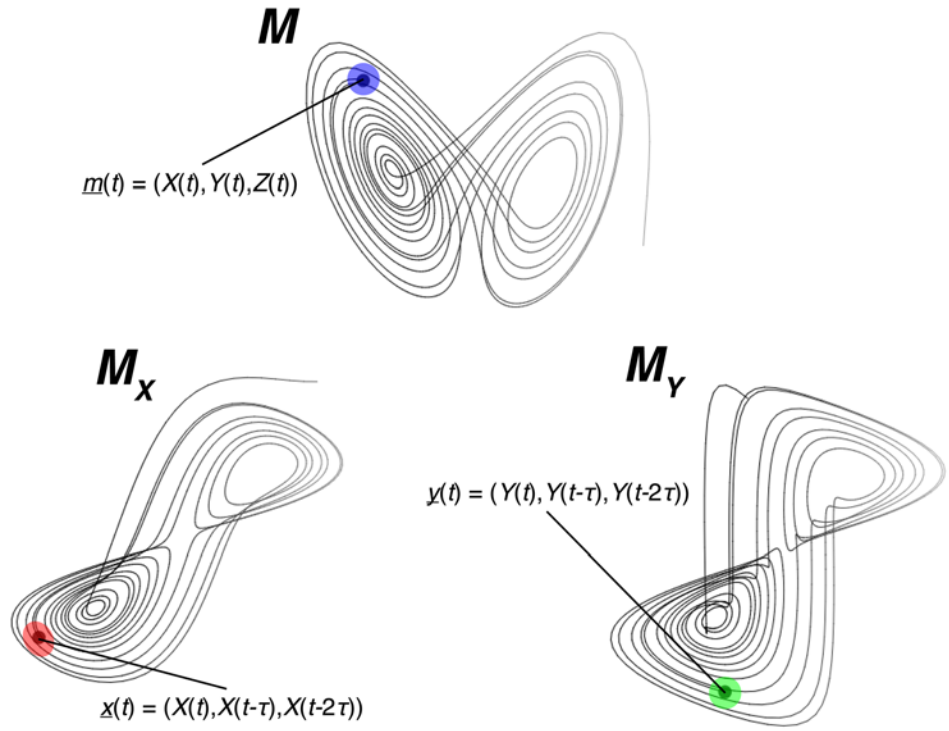

Fig. 2. Convergent cross mapping tests for correspondence between shadow manifolds. This example based on the canonical Lorenz system (a coupled system in *X*, *Y*, and *Z*; eq. S7 without *V*) shows the attractor manifold for the original system (**M**) and two shadow manifolds, $\mathbf{M}_X$ and $\mathbf{M}_Y$, constructed using lagged-coordinate embeddings of *X* and *Y*, respectively (lag = τ). Because *X* and *Y* are dynamically coupled, points that are nearby on $\mathbf{M}_X$ (e.g., within the red ellipse) will correspond temporally to points that are nearby on $\mathbf{M}_Y$ (e.g., within the green circle). That is, the points inside the red ellipse and green circle will have corresponding time indices (values for *t*). This enables us to estimate states across manifolds using *Y* to estimate the state of *X* and vice-versa using nearest neighbors (*3*). More specifically, the time indices (the values for the *t*'s) of the neighboring points of $y(t)$ on $\mathbf{M}_Y$ are used to identify the nearest neighbors of target point $x(t)$ on $\mathbf{M}_X$, and these are then averaged to estimate $x(t)$. With longer time series, the shadow manifolds become denser, and the neighborhoods (ellipses of nearest neighbors) shrink, allowing more precise cross map estimates (see movies S1 to S3).

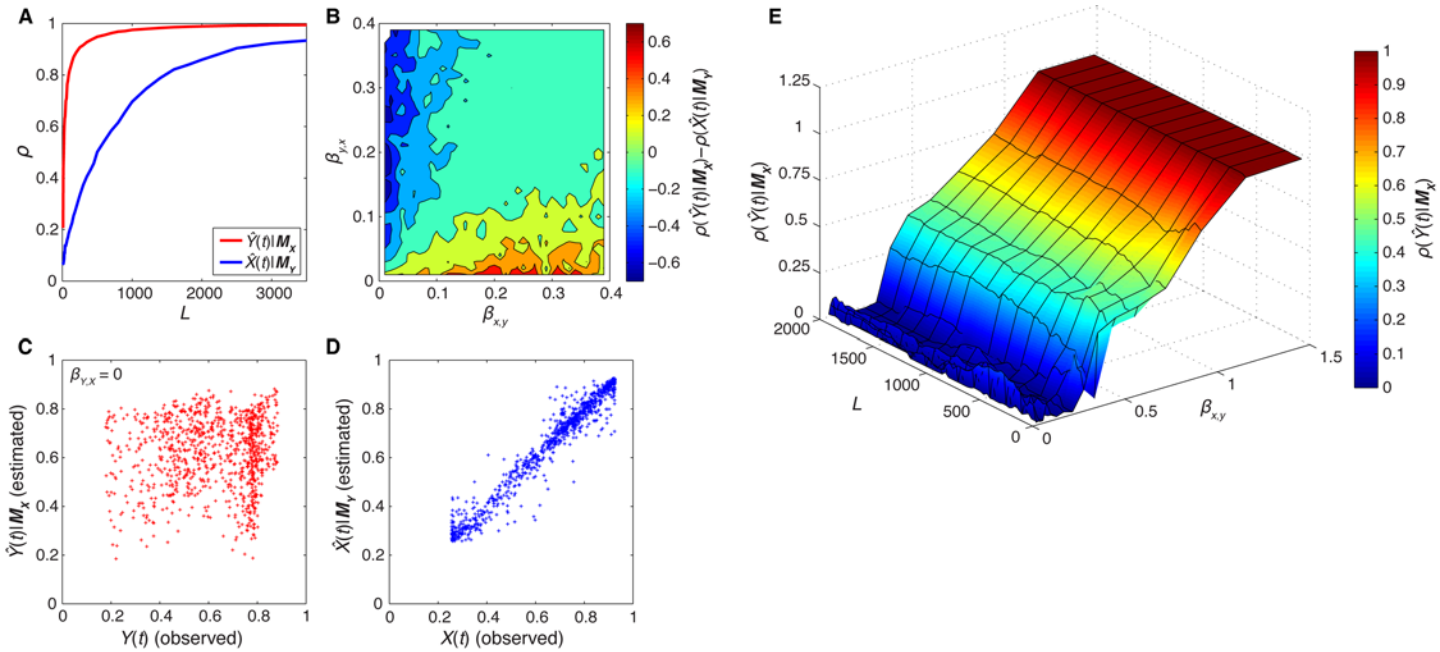

Fig. 3. Detecting causation with convergent cross mapping. (**A**) Relative convergence rates for cross mapping for the system in Fig. 1 where $\beta_{y,x} >> \beta_{x,y} > 0$. The correlation coefficient (ρ) indicates the skill of cross map estimates. With time series (libraries) of similar length, *L*, cross mapping of *Y* using $\mathbf{M}_X$, $[\hat{Y}(t)|\mathbf{M}_X]$, is stronger than cross mapping of *X* using $\mathbf{M}_Y$, $[\hat{X}(t)|\mathbf{M}_Y)]$. (**B**) Summary of this effect in general for Eq. 1. In the lower right corner where $\beta_{x,y} > \beta_{y,x}$, red regions indicate that the cross mapping of *Y* is stronger than the cross mapping of *X*: $\rho[\hat{Y}(t)|\mathbf{M}_X] > \rho[\hat{X}(t)|\mathbf{M}_Y]$. (**C**) In the extreme case where $\beta_{x,y} = 0$, *Y* (red) has no effect on *X* (blue), thus cross mapping of *Y* using $\mathbf{M}_X$ fails (ρ = 0.0). (**D**) Cross mapping of *X* succeeds because past values of *Y* contain an imprint of the dynamics of *X*. Thus, $X \Rightarrow Y$. (**E**) Demonstration of the non-convergence of $\hat{Y}(t)|\mathbf{M}_X$ as a function of forcing strength, $\beta_{x,y}$. Although partial predictability can occur when $\beta_{x,y} = 0$, this does not converge. Convergence only occurs as a special case if strong forcing causes the system to collapse dimensionality (dark red plateau at high $\beta_{x,y}$), making *X* and *Y* observation functions of the same forcing subsystem.

Fig. 4. Model causal networks. (**A**) Schematics of causal networks: two base cases and two model examples showing external forcing of non-coupled variables. (**B**) Cross mapping results for example 1: external forcing of non-coupled variables. Cross-correlation erroneously suggests that *X* and *Y* are interacting, whereas cross mapping correctly shows that there is no interaction. (**C**) Cross mapping results for the complex five-species model example. All significant ($p < 0.05$) mappings are given and indicate that species 1, 2, 3 (the subsystem in the circle) all interact mutually (case *i*), but only interact asymmetrically as external forcing variables with respect to 4 and 5 (case *ii*), which do not interact directly themselves.

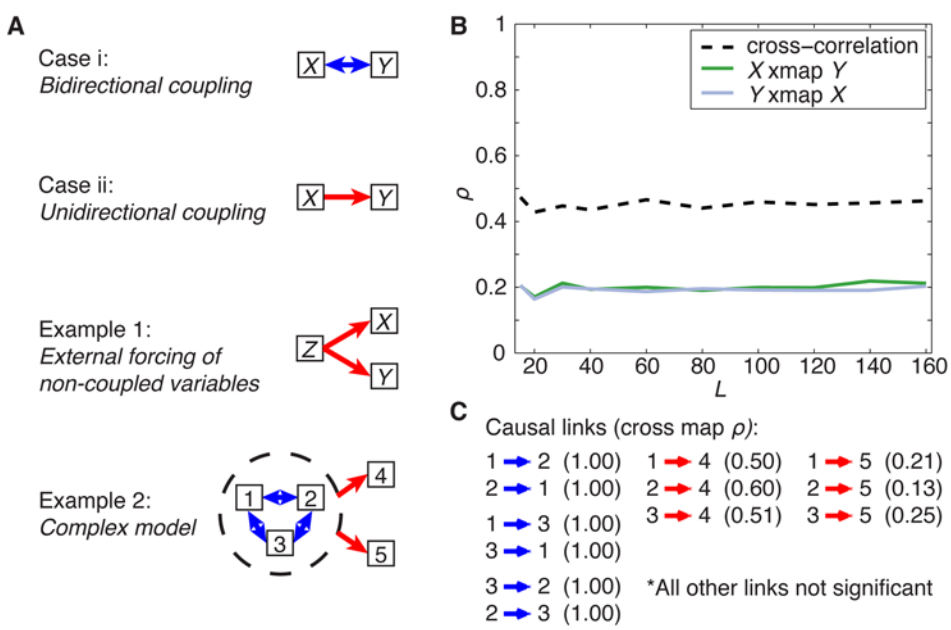

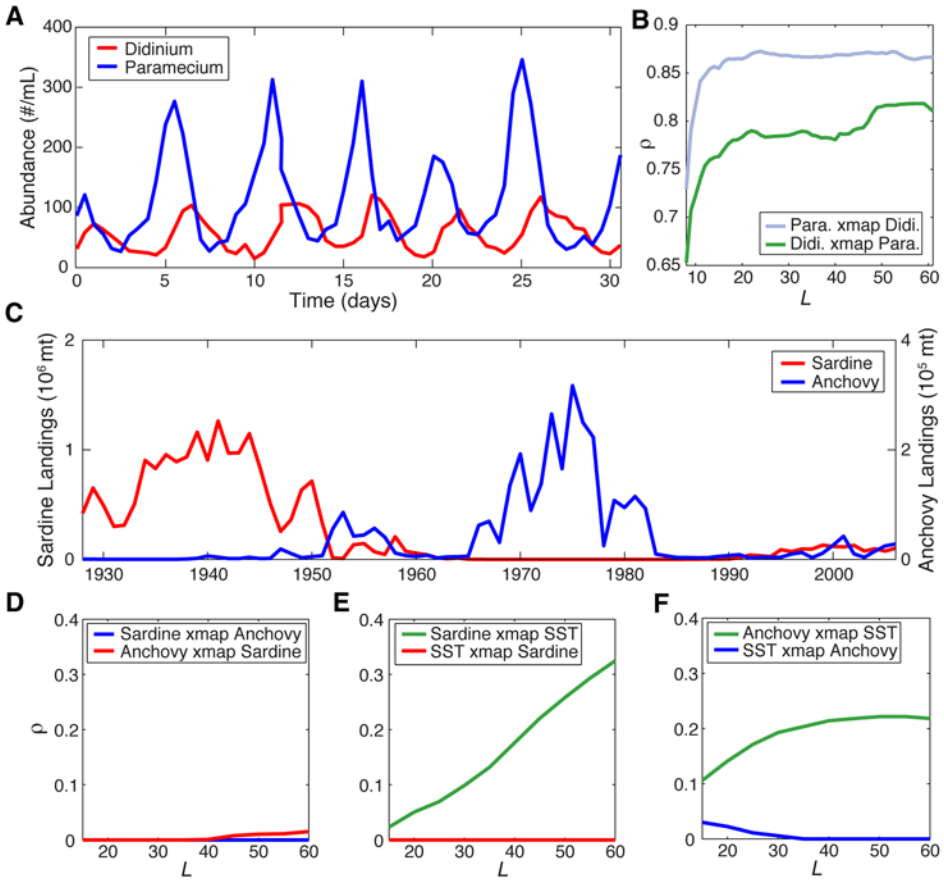

Fig. 5. Detecting causation in real time series. (**A**) Abundance time series of *Paramecium aurelia* and *Didinium nasutum* as reported in (*28*). (**B**) Convergent cross mapping of *Paramecium* and *Didinium* with increasing time series length *L*. The pattern suggests top-down predator-control. (**C**) California landings of Pacific sardine (*Sardinos sagax*) and northern anchovy (*Engraulis mordax*). (**D** to **F**) Convergent cross mapping (or lack thereof) of sardine vs. anchovy, sardine vs. SST (Scripps Pier), and anchovy vs. SST (Newport Pier), respectively. This shows that sardines do not interact with each other, but both are forced by temperature.